Synthesis and Characterization of Polyrotaxanes Consisting of Cationic α-Cyclodextrins Threaded on Poly[(ethylene oxide)-*ran*-(propylene oxide)] as Gene Carriers

Chuan Yang,[†] Xin Wang,[‡] Hongzhe Li,[‡] Suat Hong Goh,[§] and Jun Li*[,†,‡]

Division of Bioengineering, Faculty of Engineering, National University of Singapore, 7 Engineering Drive 1, Singapore 117574, Republic of Singapore, Institute of Materials Research and Engineering, National University of Singapore, 3 Research Link, Singapore 117602, Republic of Singapore, and Department of Chemistry, Faculty of Science, National University of Singapore, 3 Science Drive 3, Singapore 117543, Republic of Singapore

Received April 30, 2007; Revised Manuscript Received July 20, 2007

Cationic polymers have been receiving growing attention as gene delivery carriers. Herein, a series of novel cationic supramolecular polyrotaxanes with multiple cationic α-cyclodextrin (α-CD) rings threaded and blocked on a poly[(ethylene oxide)-*ran*-(propylene oxide)] (P(EO-*r*-PO)) random copolymer chain were synthesized and investigated for gene delivery. In the cationic polyrotaxanes, approximately 12 cationic α-CD rings were threaded on the P(EO-*r*-PO) copolymer with a molecular weight of 2370 Da and an EO/PO molar ratio of 4:1, while the cationic α-CD rings were grafted with linear or branched oligoethylenimine (OEI) of various chain lengths and molecular weights up to 600 Da. The OEI-grafted α-CD rings were only located selectively on EO segments of the P(EO-*r*-PO) chain, while PO segments were free of complexation. This increased the mobility of the cationic α-CD rings and the flexibility of the polyrotaxanes, which enhanced the interaction of the cationic α-CD rings with DNA and/or the cellular membrane. All cationic polyrotaxanes synthesized in this work could efficiently condense plasmid DNA to form nanoparticles that were suitable for delivery of the gene. Cytotoxicity studies showed that the cationic polyrotaxanes with all linear OEI chains of molecular weights up to 423 Da exhibited much less cytotoxicity than high-molecular-weight branched polyethylenimine (PEI) (25 kDa) in both HEK293 and COS7 cell lines. The cationic polyrotaxanes displayed high gene transfection efficiencies in a variety of cell lines including HEK293, COS7, BHK-21, SKOV-3, and MES-SA. Particularly, the gene delivery capability of the cationic polyrotaxanes in HEK293 cells was much higher than that of high-molecular-weight branched PEI (25 k).

1. Introduction

Over the last few decades, the development of nonviral gene carriers with low cytotoxicity and high transfection efficiency has been the hardest task for gene delivery systems, and hundreds of cationic polymers have been developed as gene carriers in numerous laboratories around the world.[1,2] In comparison with viral vectors and cationic lipids, cationic polymers for gene delivery are generally economical and stable. They can be produced on a large scale and show low host immunogenicity. So far, a great number of cationic polymers have been reported to be able to deliver genes, including homopolymers or derivatives of polyethylenimine (PEI),[3] poly(L-lysine),[4] polyamidoamine,[5] poly(L-glutamic acid),[6] polyphosphoester,[7] chitosan,[8] and cyclodextrins (CDs).[9−13]

Cyclodextrins are a series of cyclic oligosaccharides composed of 6, 7, or 8 D-(+)-glucose units linked by α-1,4-linkages and named α-, *β*-, or *γ*-CD, respectively. Recently, increasing attention has been focused on studies of supramolecular structures of polyrotaxanes formed by CDs threaded on a polymer chain[14−22] and their applications in biomaterials.[23−25] In contrast to conventional polymers containing long sequences of covalently bonded repeating units, the macrocycles in polyrotaxanes can rotate and/or slide along the polymeric chain freely.[26,27] We recently reported the synthesis of a novel cationic supramolecular structure composed of multiple oligoethylenimine (OEI)-grafted *β*-CDs that are threaded and blocked on a polymer chain as a new class of polymeric gene delivery vectors.[28] The novel supramolecular gene carriers contain many cationic cyclic units that are threaded upon a polymer chain to form an integrated supramolecular entity to function as a macromolecular gene vector, which showed excellent DNA binding ability, low cytotoxicity, and high gene transfection efficiency in HEK293 cells. Yui and co-workers also reported the use of dimethylaminoethyl-modified α-CDs threaded onto a poly(ethylene oxide) (PEO) chain and capped by cleavable end groups for gene delivery.[29] The cleavage of the end groups caused the dethreading of α-CDs and a rapid release of DNA in cells, but the tertiary amine conjugated to the α-CD rings might not be efficient in DNA complexation and gene delivery.

We previously found that a random copolymer, poly[(ethylene oxide)-*ran*-(propylene oxide)] (P(EO-*r*-PO)), can form inclusion complexes with α-CD.[30] Although there are propylene oxide (PO) units randomly placed in the polymer backbone, the copolymer still can penetrate the smallest cavity of α-CD to form inclusion complexes. It was concluded that α-CD can overcome the energy barrier in passing over a PO unit or a short PO segment and then form a stable inclusion complex with

* Author to whom correspondence should be addressed. Phone: +65-6516-7273. Fax: +65-6872-3069. E-mail: bielj@nus.edu.sg.
† Division of Bioengineering, Faculty of Engineering.
‡ Institute of Materials Research and Engineering.
§ Department of Chemistry, Faculty of Science.

10.1021/bm700472t CCC: $37.00
Published on Web 10/12/2007

Scheme 1. Synthesis Procedures and Structures of Multiple OEI-Grafted Cationic Polyrotaxanes (**5a**, **5b**, **5c**, and **5d**)

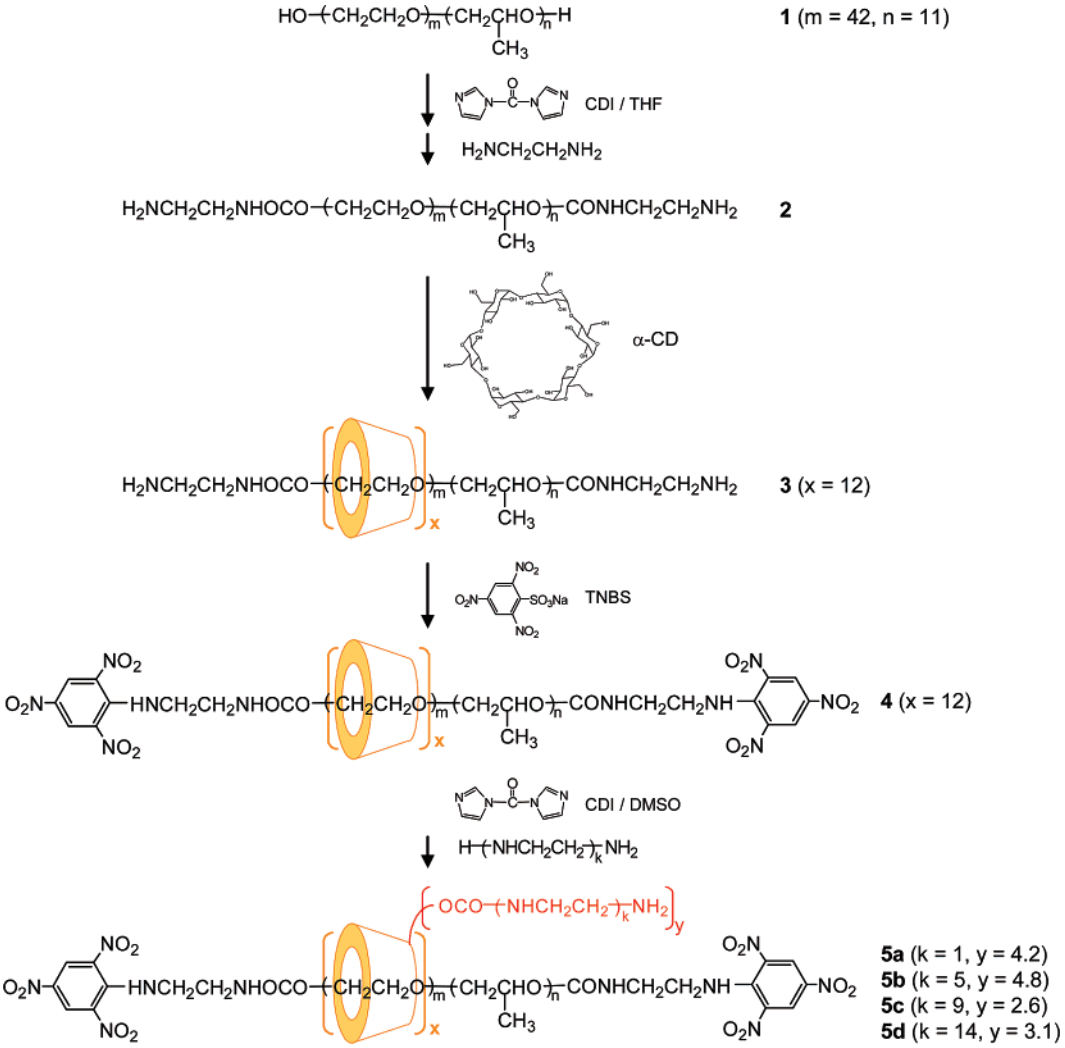

ethylene oxide (EO) units of the copolymer. In this paper, we report the synthesis and characterization of a series of polyrotaxanes consisting of multiple cationic α-CD rings threaded on a P(EO-*r*-PO) copolymer as new gene carriers. The design of the gene carriers was based on the inclusion complex formation between α-CD and the P(EO-*r*-PO) copolymer. In the polyrotaxane gene carriers, the cationic α-CD rings only resided selectively on the EO segments of the P(EO-*r*-PO) chain, which may increase the mobility of α-CD rings through rotating and/or sliding along the copolymer as well as the flexibility of the polyrotaxane, enhancing the interaction of the cations of α-CD rings with DNA and/or the cellular membranes. The polyrotaxane gene carriers showed high transfection efficiencies in a variety of cell lines, while exhibiting much lower cytotoxicity than branched high-molecular-weight PEI.

2. Materials and Methods

2.1. Materials. The P(EO-*r*-PO) copolymer (M_n = 2370 Da, M_w/M_n =1.06) was supplied by Aldrich. This copolymer had a chain composition of $EO_{41}PO_{10}$. The molecular characteristics, which were found to be within the specifications of the supplier, were confirmed using gel permeation chromatography (GPC) and ^{1}H NMR spectroscopy. 2,4,6-Trinitrobenzene sulfonic acid (TNBS) solution and pentaethylenehexamine (OEI-5) were obtained from Fluka. 1,1′-Carbonyldiimidazole (CDI) and α-cyclodextrin were purchased from Tokyo Kasei, Inc. Ethylenediamine (OEI-1), linear PEI with a molecular weight of 423 Da (OEI-9), branched PEI with a molecular weight of 600 Da (OEI-14), and branched PEI (molecular weight 25 kDa) were supplied by Aldrich. DMSO-d_6 and D_2O used as solvents in the NMR measurements were obtained from Aldrich. The Qiagen kit and Luciferase kit were purchased from Qiagen and Promega, respectively. 3-(4,5-Dimethyl-thiazol-2-yl)-2,5-diphenyl tetrazodium bromide (MTT), penicillin, and streptomycin were obtained from Sigma.

2.2. Synthesis. The procedures for the synthesis of polyrotaxanes consisting of multiple cationic α-CD rings threaded on the P(EO-*r*-PO) copolymer are shown in Scheme 1. The following describes the details of the synthesis of **5b** from P(EO-*r*-PO) copolymer **1** as a typical example.

2.2.1. P(EO-r-PO)−Bis(amine) 2. P(EO-*r*-PO) copolymer **1** (M_n = 2370 Da, 1.90 g, 0.80 mmol) was heated in a flask at 80 °C under vacuum overnight. After the flask cooled, 15 mL of anhydrous dimethylformamide (DMF) was injected under nitrogen. After all of **1** was dissolved, the DMF solution of **1** was added dropwise during a period of 6 h under nitrogen to 15 mL of anhydrous DMF solution in which CDI (1.30 g, 8.0 mmol) was dissolved, and the mixture was stirred overnight under nitrogen at room temperature. Then, the resulting solution was slowly added dropwise during a period of 3 h into 4.8 g (80 mmol) of ethylenediamine that was dissolved in 15 mL of anhydrous DMF with stirring at room temperature, followed by stirring the mixture overnight. Excess ethylenediamine and DMF were removed by vacuum evaporation. The resulting viscous solution was purified by size exclusion chromatography (SEC) on a Sephadex LH-20 column using methanol as the eluent. Finally, 1.42 g of viscous liquid **2** was obtained (yield, 70%). ^{1}H NMR (400 MHz, DMSO-d_6, 22 °C, δ):

3.25−3.71 (m, 168H and 33H, methylene of EO segments and methylene and methine of PO segments), 3.23 (s, 4H, $-CH_2-$ of $-CONHCH_2-$), 2.01 (s, 4H, $-CH_2-$ of $-CH_2NH_2$), 1.06 (d, 33H, $-CH_3$ of PO segments).

*2.2.2. Polyrotaxane **4**.* P(EO-*r*-PO)−bis(amine) **2** (0.20 g) was added to 27.6 mL of an α-CD saturated aqueous solution (0.145 g/mL) that contained 0.30 g of $NaHCO_3$ for adjustment of the pH value of the solution. The reaction mixture was ultrasonicated for 20 min and stirred at room temperature overnight. Then, 0.55 g of the sodium salt of TNBS was added and stirred overnight, followed by pouring 100 mL of water into the reaction mixture. The precipitate was centrifuged and washed with water three times. The resulting wet solid was dissolved in 20 mL of dimethylsulfoxide (DMSO) and poured into 300 mL of MeOH to precipitate the product. The precipitate was centrifuged and washed with MeOH three times. The resulting wet solid was dissolved in 20 mL of DMSO again and poured into 300 mL water to precipitate the product. The resulting precipitate was centrifuged and washed with water three times. Finally, the resulting wet solid was freeze-dried, and 0.59 g of pure polyrotaxane **4** was obtained (yield, 52%). ^{1}H NMR (400 MHz, DMSO-d_6, 22 °C, δ): 8.93 (broad, s, 4H, meta H of phenyl), 5.63 (s, 66H, O(2)H of CD), 5.47 (m, 66H, O(3)H of CD), 4.75 (s, 66H, H(1) of CD), 4.41 (s, 66H, O(6)H of CD), 3.17−3.840 (m, 396H, H(3), H(6), H(5), H(2), and H(4) of CD; 168H, methylene of EO segments; 33H, methylene and methine of PO segments), 1.07 (broad, s, 33H, $-CH_3$ of PO segments).

*2.2.3. Cationic Polyrotaxane **5b**.* The resulting polyrotaxane **4** (0.206 g, 0.015 mmol) was dried in a flask at 40 °C under vacuum overnight. After the flask cooled, 40 mL of anhydrous DMSO was injected under nitrogen. After all of **4** was dissolved, the DMSO solution of **4** was added dropwise during a period of 6 h under nitrogen to 40 mL of anhydrous DMSO solution in which CDI (2.56 g, 16.35 mmol) was dissolved, and the mixture was stirred overnight under nitrogen at room temperature. A mixture of tetrahydrofuran (THF) (300 mL) and Et_2O (600 mL) was poured into the resulting solution to precipitate the product. The precipitate was centrifuged and washed with THF three times. Then, the resulting wet solid was dissolved in 40 mL of anhydrous DMSO, and this solution was slowly added dropwise during a period of 3 h into 5.70 mL (19.62 mmol) of pentaethylenehexamine that was dissolved in 40 mL of anhydrous DMSO while stirring at room temperature, followed by stirring the mixture overnight. THF (900 mL) was poured into the reaction mixture to precipitate the product. The precipitate was centrifuged and washed with THF three times, and the resulting crude product was purified by SEC on a Sephadex G-50 column using deionized water as the eluent. Finally, 0.169 g of brown solid **5b** was obtained (yield, 41%).

The yields and analytical data for all four cationic polyrotaxanes synthesized in this work are given below.

*2.2.4. Cationic Polyrotaxane **5a**.* Yield, 35%. ^{1}H NMR (400 MHz, D_2O, 22 °C, δ): 8.38 (s, 2H, meta H of phenyl), 7.99 (s, 2H, meta H of phenyl), 5.03 (s, broad, 66H, H(1) of CD), 2.95−4.61 (m, broad, 396H, H(3), H(6), H(5), H(2), and H(4) of CD; 168H, methylene of EO segments; 33H, methylene and methine of PO segments; 138H, methylene of $-CONHCH_2-$), 2.78 (s, 138H, methylene of $-CH_2NH_2$), 1.08 (d, 33H, $-CH_3$ of PPO block).

*2.2.5. Cationic Polyrotaxane **5b**.* Yield, 41%. ^{1}H NMR (400 MHz, D_2O, 22 °C, δ): 8.36 (s, 2H, meta H of phenyl), 7.97 (s, 2H, meta H of phenyl), 4.95 (s, broad, 66H, H(1)H of CD), 2.94−4.58 (m, broad, 396H, H(3), H(6), H(5), H(2), and H(4) of CD; 168H, methylene of EO segments; 33H, methylene and methine of PO segments; 106H, methylene of $-CONHCH_2-$), 2.67 (m, 1268H, methylene of pentaethylenehexamine), 1.07 (s, 33H, $-CH_3$ of PO segments).

*2.2.6. Cationic Polyrotaxane **5c**.* Yield, 30%. ^{1}H NMR (400 MHz, D_2O, 22 °C, δ): 8.37 (s, 2H, meta H of phenyl), 7.98 (s, 2H, meta H of phenyl), 4.98 (d, broad, 66H, H(1)H of CD), 2.97−4.62 (m, broad, 396H, H(3), H(6), H(5), H(2), and H(4) of CD; 168H, methylene of EO segments; 33H, methylene and methine of PO segments; 57H, methylene of $-CONHCH_2-$), 2.67 (m, 1305H, methylene of OEI-9), 1.08 (d, 33H, $-CH_3$ of PO segments).

*2.2.7. Cationic Polyrotaxane **5d**.* Yield, 48%. ^{1}H NMR (400 MHz, D_2O, 22 °C, δ): 8.36 (s, 2H, meta H of phenyl), 7.98 (s, 2H, meta H of phenyl), 4.98 (d, broad, 66H, H(1)H of CD), 2.97−4.61 (m, broad, 396H, H(3), H(6), H(5), H(2), and H(4) of CD; 168H, methylene of EO segments; 33H, methylene and methine of PO segments; 69H, methylene of $-CONHCH_2-$), 2.56 (m, 1293H, methylene of OEI-14), 1.09 (d, 33H, $-CH_3$ of PO segments).

2.3. Analytical methods. GPC analysis for the P(EO-*r*-PO) copolymer was carried out with a Shimadzu SCL-10AVP and LC-10ATVP system equipped with two Phenogel 5 μm, 50, and 1000 Å columns (size, 300 mm × 4.6 mm) in series and a Shimadzu RID-10A refractive index (RI) detector. THF was used as the eluent at a flow rate of 0.30 mL/min at 40 °C. Monodispersed poly(ethylene glycol) standards were used to obtain a calibration curve.

SEC analysis for cationic polyrotaxanes was carried out with a Shimadzu SCL-10AVP and LC-10ATVP system equipped with a Sephadex G-75 column (size, 2.5 cm × 32 cm), a Shimadzu RID-10A RI detector, and a Shimadzu SPD-10Avp UV−vis detector. Phosphate-buffered saline (PBS) solution (1×) was used as the eluent. One milliliter fractions were collected, and their optical rotations (ORs) were further measured using a HORIBA SEPA-300 high speed accurate polarimeter at a wavelength of 589 nm with a cell length of 10 cm and response time of 2 s.

The ^{1}H NMR spectra were recorded on a Bruker AV-400 NMR spectrometer at 400 MHz at room temperature. The ^{1}H NMR measurements were carried out with an acquisition time of 3.2 s, a pulse repetition time of 2.0 s, a 30° pulse width, a 5208 Hz spectral width, and 32 000 data points. Chemical shifts were referred to the solvent peaks (δ = 4.70 ppm for D_2O and 2.50 ppm for DMSO-d_6).

The ^{13}C NMR spectra were recorded on a Bruker AV-400 NMR spectrometer at 100 MHz at room temperature. The ^{13}C NMR measurements were carried out using composite pulse decoupling with an acquisition time of 0.82 s, a pulse repetition time of 5.0 s, a 30° pulse width, a 20 080 Hz spectral width, and 32 000 data points. The chemical shifts were referred to an external standard.

2.4. Plasmid. The plasmid used was pRL-CMV (Promega, Madison, WI), encoding *Renilla* luciferase, which was originally cloned from the marine organism *Renilla reniformis*. The plasmid DNA was amplified in *Escherichia coli* and purified according to the supplier's protocol (Qiagen, Hilden, Germany). The purity and concentration of the purified plasmid DNA were determined by absorption at 260 and 280 nm and by agarose gel electrophoresis. The purified plasmid DNA was resuspended in TE buffer (10 mM Tris-Cl, pH 7.5, 1 mM EDTA) and kept in aliquots at a concentration of 0.5 mg mL^{-1}.

2.5. Cells and Media. All cell lines were purchased from the American Type Culture Collection (Rockville, MD). COS7, HEK293, and BHK-21 cells were maintained in Dulbecco's modified Eagle's medium (DMEM supplemented with 10% heat-inactivated fetal bovine serum (FBS), 100 units/mg penicillin, and 100 μg/mL streptomycin at 37 °C and 5% CO_2. MES-SA and SKOV-3 cells were grown in McCoy's 5a medium with 1.5 mM L-glutamine supplemented with 10% heat-inactivated FBS, 100 units/mg penicillin, and 100 μg/mL streptomycin at 37 °C and 5% CO_2. Reduced-serum Opti-MEM medium, DMEM medium, and McCoy's 5a medium were purchased from Gibco BRL (Gaithersburg, MD).

2.6. Gel Retardation Experiments. Each polymer was examined for its ability to bind pRL-CMV plasmid DNA through agarose gel electrophoresis experiments. All polymer stock solutions were prepared at a nitrogen concentration of 1 mM in distilled water, and the pH was adjusted to 7.4. pRL-CMV (0.2 μg in 2 μL of TE buffer) was mixed with polymer at nitrogen/phosphate (N/P) ratios from 0 to 10. Each mixture was vortexed and incubated for approximately 30 min at room temperature and then analyzed on a 1% agarose gel containing 0.5 μg/mL ethidium bromide (EtBr). The gel electrophoresis was carried out in TAE running buffer (40 mM Tris-acetate, 1 mM EDTA) for 40 min

at 80 V in a Sub-Cell system (Bio-Rad Laboratories, Hercules, CA). The DNA bands were visualized and photographed by a UV transilluminator and BioDoc-It imaging system (UVP Inc., Upland, CA).

2.7. Cell Viability Assay. The cytotoxicity of the cationic polyrotaxanes in comparison with PEI (25 kDa) was evaluated using the MTT assay in COS7 and HEK293 cell lines. The cells were cultured in complete DMED medium supplemented with 10% FBS at 37 °C, 5% CO_2, and 95% relative humidity. The cells were seeded in a 96-well microtiter plate (Nunc, Wiesbaden, Germany) at densities of 10 000 and 15 000 cells/well for COS7 and HEK293, respectively. After 24 h, culture media were replaced with serum-supplemented culture media containing serial dilutions of polymers, and the cells were incubated for 24 h. Then, 10 μL of sterile-filtered MTT stock solution in PBS (5 mg/mL) was added to each well, reaching a final MTT concentration of 0.5 mg/mL. After 5 h, unreacted dye was removed by aspiration. The formazan crystals were dissolved in DMSO (100 μL/well), and the absorbance was measured using a microplate reader (Spectra Plus, TECAN) at a wavelength of 570 nm. The relative cell viability (%) related to control cells cultured in media without polymers was calculated with $[A]_{test}/[A]_{control} \times 100\%$, where $[A]_{test}$ is the absorbance of the wells with polymers and $[A]_{control}$ is the absorbance of the control wells. All experiments were conducted for six samples and averaged. The median lethal dose (LD_{50}) is the dose of a toxic material that kills half (50%) of the cells tested. In this study, LD_{50} was the concentration of a gene carrier at which the relative cell viability decreased to 50%.

2.8. In Vitro Transfection and Luciferase Assay. Transfection studies were performed in five cell lines (HEK293, COS7, BHK-21, MES-SA, and SKOV-3 cells) using the plasmid pRL-CMV as the reporter gene. In brief, 24 h before transfection, 24-well plates were seeded with cells at a density of 5×10^4/well. The polymer/DNA complexes (2.0 μg DNA/well for HEK293 and COS7 cells and 1.0 μg DNA/well for the other cell lines) at various N/P ratios were prepared by adding the polymer into DNA solutions dropwise, followed by vortexing and incubation for 30 min at room temperature before the transfection. At the time of transfection, the medium in each well was replaced with reduced-serum Opti-MEM medium or normal complete DMEM medium. The complexes were added into the transfection medium and incubated with cells for 4 h under standard incubator conditions. After 4 h, the medium was replaced with 500 μL of fresh medium supplemented with 10% FBS, and the cells were further incubated for an additional 20 h under the same conditions, resulting in a total transfection time of 24 h. Cells were washed with PBS twice, and lysed in 100 μL of cell culture lysis reagent (Promega, Cergy Pontoise, France). Luciferase gene expression was quantified using a commercial kit (Promega, Cergy Pontoise, France) and a luminometer (Berthold Lumat LB 9507, Germany). Protein concentration in the samples was analyzed using a bicinchoninic acid assay (Bio-Rad Laboratories, Hercules, CA). Absorption was measured on a microplate reader (Spectra Plus, TECAN) at 570 nm and compared to a standard curve calibrated with bovine serum albumin samples of known concentrations. Results are expressed as relative light units per milligram of cell protein lysate (RLU mg^{-1} protein).

2.9. Dynamic Light Scattering and Zeta-Potential Measurements. Measurements of particle size and zeta potential of the complexes were performed using a Zetasizer Nano ZS (Malvern Instruments, Southborough, MA) with a laser light wavelength of 633 nm at a 173° scattering angle. Complex solutions (100 μL) containing 3 μg of pDNA (pRL-CMV) were prepared at various N/P ratios ranging from 2 to 30. The mixture was vortexed for 20 s, incubated for 30 min at room temperature, and diluted in 1 mL of distilled water before being analyzed on the Zetasizer. The size measurement was performed at 25 °C in triplicate. The deconvolution of the measured correlation curve to an intensity size distribution was accomplished using a non-negative least-squares algorithm. The *Z*-average hydrodynamic diameters of the particles were given by the instrument. The *Z*-average size is the intensity-weighted mean diameter derived from a cumulants or single-exponential fit of the intensity autocorrelation function. The zeta-potential measurements were performed using a capillary zeta-potential cell in automatic mode using the same samples for the particle size measurements.

2.10. Atomic Force Microscopy. A Digital Instruments MultiMode atomic force microscope with a Nanoscope IV controller in tapping mode was employed to image the nanoparticle samples. Briefly, silicon disks were soaked in 50% acetone for a minimum of 2 h and rinsed with distilled water. When the silicon disks were completely dried, 20 μL of cationic polyrotaxane **5c**/DNA complexes containing 1.0 μg of pRL-CMV at N/P ratios 0, 2, and 10 was placed on the silicon surface for 2 min, followed by removal of the complex solutions carefully with a piece of tissue paper. All of the atomic force microscopy (AFM) images were obtained with a scan rate of 0.5 or 1 Hz over a selected area of 2 μm × 2 μm. Image analysis was performed using Nanoscope software after removal of the background slope by flattening images.

2.11. Confocal Microscopy. For confocal microscopy imaging of the gene transfection, the plasmid pEGFP-N1 (Clontech Laboratories, Inc., Mountain View, CA), encoding a red-shifted variant of wild-type green fluorescence protein (GFP), was used to examine the GFP expression in HEK293 cells. HEK293 cells were seeded onto a Lab-Tek four-chambered coverglass (Nalge-Nane International, Naperville, IL) at a density of 5×10^4 cells/well in 500 μL of complete DMEM medium. After 24 h, transfection was undertaken with 2 μg of EGFP plasmid in 0.3 mL of reduced-serum Opti-MEM medium in each well. At the time of transfection, 20 μL of cationic polyrotaxane **5c**/DNA complex solution was added in each well. After 4 h, the transfection medium was removed, and the cells were washed with fresh complete DMEM medium. After 20 h of further incubation in serum containing complete DMEM medium, the cells were washed with PBS and imaged under a laser scanning confocal microscope (LSM 410, Carl Zeiss, Göttingen, Germany). GFP fluorescence was excited at 488 nm, and emission was collected using a 515 nm filter.

3. Results and Discussion

3.1. Synthesis of Cationic Polyrotaxanes. Scheme 1 shows the synthesis procedures and the structures of the cationic polyrotaxanes (**5a**, **5b**, **5c**, and **5d**). First, P(EO-*r*-PO)−bis(amine) **2** was prepared from P(EO-*r*-PO) random copolymer **1,** which has a number-average molecular weight (MW) of 2370 Da and an 80 mol % content of EO segments. The two hydroxy end groups were activated with CDI, followed by reaction with excess ethylenediamine to give **2**. We previously reported that P(EO-*r*-PO) can form inclusion complexes with α-CD, although there are PO segments randomly placed in the copolymer backbone, and a PPO homopolymer cannot form a complex with α-CD because the PPO chain is too large to penetrate the small inner cavity of α-CD.[30] We interestingly found that α-CD molecules are able to overcome the energy barrier in passing over a PO unit or a short PO segment and then form a stable inclusion complex with EO segments of the P(EO-*r*-PO) random copolymer.

Polypseudorotaxane **3** was formed between P(EO-*r*-PO)−bis(amine) **2** and α-CD, and polyrotaxane **4** was synthesized by adding TNBS to **3**, forming two bulky stoppers to block the two ends of the inclusion complex, in which about 12 α-CD rings are trapped on the copolymer chain. Finally, linear or nonlinear OEIs with different MWs, ethylenediamine ($k = 1$), pentaethylenehexamine ($k = 5$), linear OEI with a MW of 423 Da (OEI-9, $k = 9$), and branched OEI with a MW of 600 Da (OEI-14, $k = 14$), were grafted to the α-CD molecules of polyrotaxane **4** to give cationic polyrotaxanes **5a**, **5b**, **5c**, and **5d**, respectively.

3.2. Molecular Characterization of Cationic Polyrotaxanes. Figure 1 shows the SEC profiles of the cationic polyrotaxanes in comparison with pristine α-CD. The elution curves for all four cationic polyrotaxanes were recorded against RI,

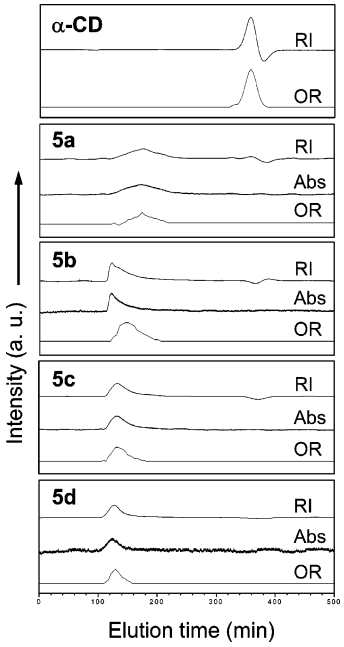

Figure 1. Size exclusion chromatograms of pristine α-CD and cationic polyrotaxanes **5a**, **5b**, **5c**, and **5d** detected using refractive index (RI), UV−vis absorption (Abs) at 419 nm, and optical rotation (OR).

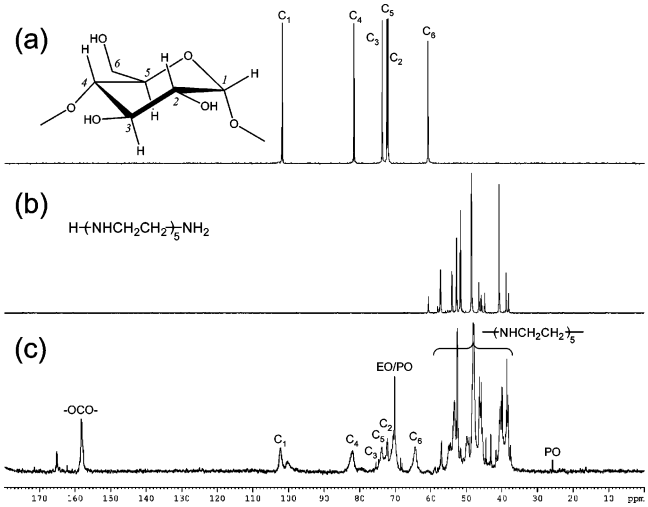

Figure 2. ^{13}C NMR spectra of (a) pristine α-CD, (b) pentaethylenehexamine, and (c) cationic polyrotaxanes **5b** in D_2O.

UV−vis absorption (Abs) at 419 nm, and OR, while that for pristine α-CD was recorded against RI and OR because it has no UV−vis absorption. As shown in Figure 1, α-CD has a relatively small molecular size, so it was eluted at the low-MW region of the column. In contrast, all four cationic polyrotaxanes were eluted out at the higher-MW region of the column due to their larger molecular sizes and were detected by RI, Abs, and OR at the same time, indicating that the cationic polyrotaxanes comprise the 2,4,6-trinitrophenyl (TNP) ends and cationic α-CD units. In comparison to the other synthetic polyrotaxanes, **5a** was eluted a bit later, which corresponds to its smaller molecular size than the other cationic polyrotaxanes, because **5a** is grafted with the shortest ethylenediamine chains. Each cationic polyrotaxane showed a single peak in the SEC profiles, indicating that the cationic polyrotaxanes are pure and there was no intra- or intermolecular cross-linking.

Figure 2 shows the ^{13}C NMR spectra of cationic polyrotaxane **5b** in comparison with pristine α-CD and pentaethylenehexamine. In Figure 2c, all peaks attributed to α-CD, the grafting OEI, and the threading copolymer were observed clearly, and the peaks were broadened because all components of the cationic polyrotaxane formed an integrated macromolecular system, which restricts their molecular motion. The peak at δ 158.1 ppm corresponds to the carbon of carbonyl groups, which links the OEI chains to α-CD rings. In comparison to pristine α-CD, the peak of C-6 of α-CD in **5b** shifted from 60.8 to 64.4 ppm. This is evidence that the grafting of OEI chains mainly happened at

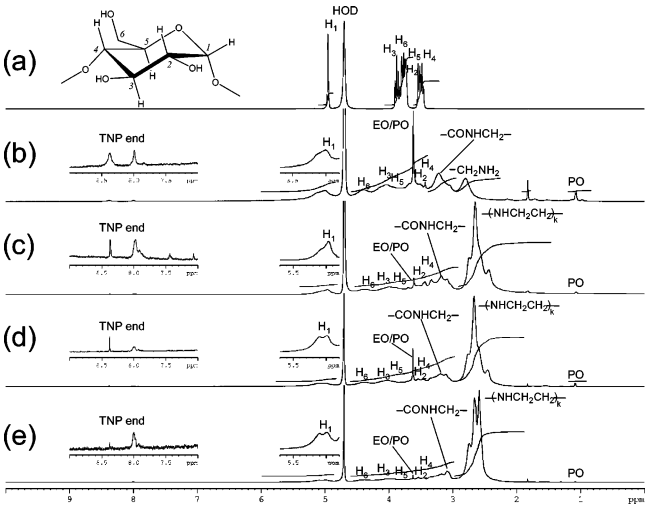

Figure 3. ^{1}H NMR spectra of (a) pristine α-CD and cationic polyrotaxanes (b) **5a**, (c) **5b**, (d) **5c**, and (e) **5d** in D_2O.

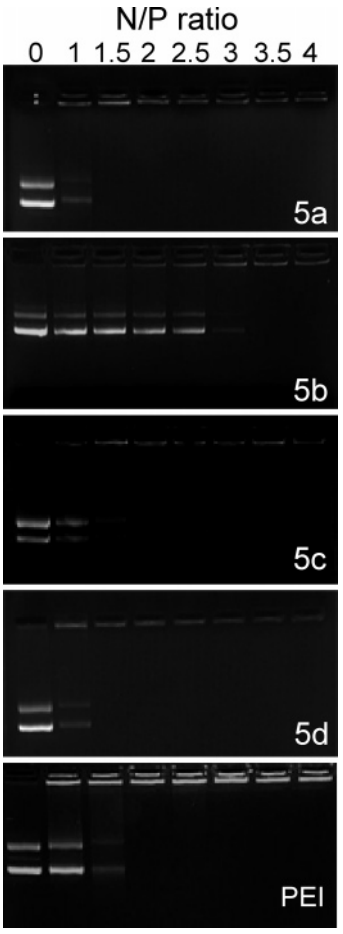

Figure 4. Electrophoretic mobility of plasmid DNA in the complexes between cationic polyrotaxanes and DNA in comparison with PEI (25 kDa)/DNA complexes at various N/P ratios.

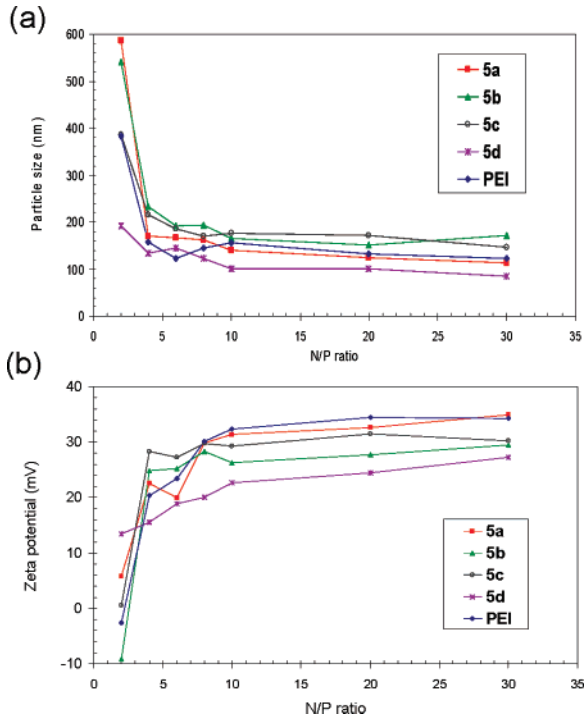

Figure 5. (a) Particle size and (b) zeta potential of the complexes between cationic polyrotaxanes and DNA in comparison with PEI (25 kDa)/DNA complexes at various N/P ratios.

the 6-position hydroxyl groups. In fact, of the three types of hydroxyl groups of α-CD, those at the 6-position (primary hydroxyl groups) are the most nucleophilic and are thought to be modified under the weak basic conditions.[31]

Figure 3 shows the ^{1}H NMR spectra of the cationic polyrotaxanes in comparison with pristine α-CD. In spectra b−e in Figure 3, the signals for α-CD, the grafting OEI chains, the threading copolymer, and the TNP ends were observed, while the peaks were much broadened due to the restriction of the molecular motion by molecular interlocking and the grafting of the OEI units. From the ^{1}H NMR spectra, the average number of OEI chains grafted to each α-CD (*y*) was estimated. Corresponding to cationic polyrotaxane **5a**, **5b**, **5c,** and **5d**, the number of OEI chains grafted to one α-CD molecule in these cationic polyrotaxanes is about 4.2, 4.8, 2.6, and 3.1, respectively. Generally, the longer the OEI chain, the fewer OEI chains could be grafted to each α-CD ring due to the influence of the steric hindrance of OEI chains on the grafting reaction. However, for **5d**, more primary amino groups from the branched structure of OEI-14 could participate in the grafting reaction, resulting in the increasing number of OEI chains grafted to each α-CD ring.

3.3. Formation of Cationic Polyrotaxane/DNA Complexes. The ability of the cationic polyrotaxanes to condense plasmid DNA (pDNA) into particulate structures was confirmed by agarose gel electrophoresis, particle size and zeta-potential measurements, as well as AFM images.

DNA condensation capability is a prerequisite for polymeric gene vectors. In this study, the complexation of cationic polyrotaxanes with DNA was analyzed using agarose gel electrophoresis. Figure 4 shows the gel retardation results of cationic polyrotaxane/DNA complexes with increasing N/P ratios in comparison with the branched PEI (25 kDa)/DNA complex. Cationic polyrotaxanes **5a**, **5c,** and **5d** could compact pDNA entirely at the low N/P ratio of 1.5−2.0, while PEI (25 kDa) could inhibit the migration of pDNA at N/P ratios of 2 and above, indicating that these polyrotaxanes have slightly better DNA condensation abilities than PEI (25 kDa). Different from the other cationic polyrotxanes, **5b** showed a lower ability to condense DNA because the migration of DNA was only retarded at N/P ratios of 3 and above.

Figure 5 shows the particle size and zeta potential measurements of cationic polyrotaxane/DNA complexes in comparison with the PEI (25 kDa)/DNA complexes at various N/P ratios. In Figure 5a, all four cationic polyrotaxanes could efficiently compact pDNA into small nanoparticles. The diameters of the complexes formed by **5a**, **5b,** and **5c** with DNA decreased sharply from more than 500 nm to around 200 nm with the increase of the N/P ratio from 2 to 4, similar to the case of the PEI (25 kDa)/DNA complex. The hydrodynamic size of the **5d**/DNA complex only varied within the range of 100−200 nm with the increase of the N/P ratio from 2 to 30. After the N/P ratio reached 6, all four cationic polyrotaxanes and PEI (25 kDa) could condense DNA into nanoparticles with diameters ranging from 100 to 200 nm.

Zeta potential is an indicator of the surface charge of polymer/DNA naoparticles, and a positive surface charge allows an electrostatic interaction between negatively charged cellular membranes and the positively charged complexes.[32] As shown in Figure 5b, the surface net charge of the complexes of pDNA with PEI (25 kDa) and cationic polyrotaxanes **5a**, **5b**, or **5c** increased dramatically as the N/P ratio increased from 2 to 4 and stabilized at N/P ratios of 10 and above. The zeta potential of the **5d**/DNA complex only varied within the range of 13−27 mV with the increase of the N/P ratio from 2 to 30. After the N/P ratio reached 10, the zeta potential of the complexes of pDNA with all four cationic polyrotaxanes and PEI (25 kDa) was strongly positive and varies within the same range (20−30 mV), which results in a similar affinity for the cell surface.[33]

Figure 6 shows representative tapping mode AFM images of naked pDNA and cationic polyrotaxane **5c**/DNA complexes at N/P ratios of 2 and 10. The images obtained clearly demonstrate significant morphological differences when different N/P ratios were applied as well as the formation of compact nanoparticles. In Figure 6a, loose, supercoiled structure of pDNA could be observed when pDNA was not condensed by a cationic polymer. At a N/P ratio of 2, supercoiled plasmid pDNA could

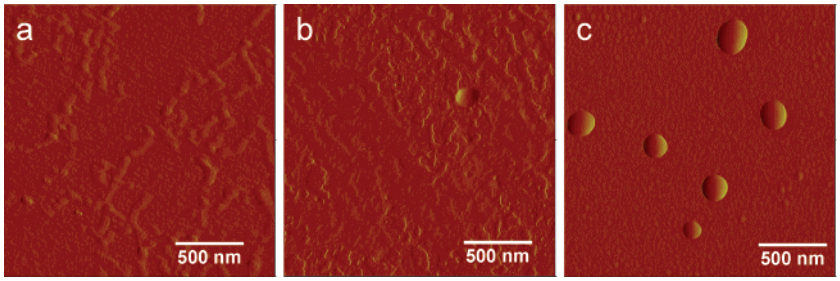

Figure 6. Atomic force microscopy images of the (a) supercoiled pDNA and cationic polyrotaxane **5c**/DNA complexes at N/P ratios of (b) 2 and (c) 10.

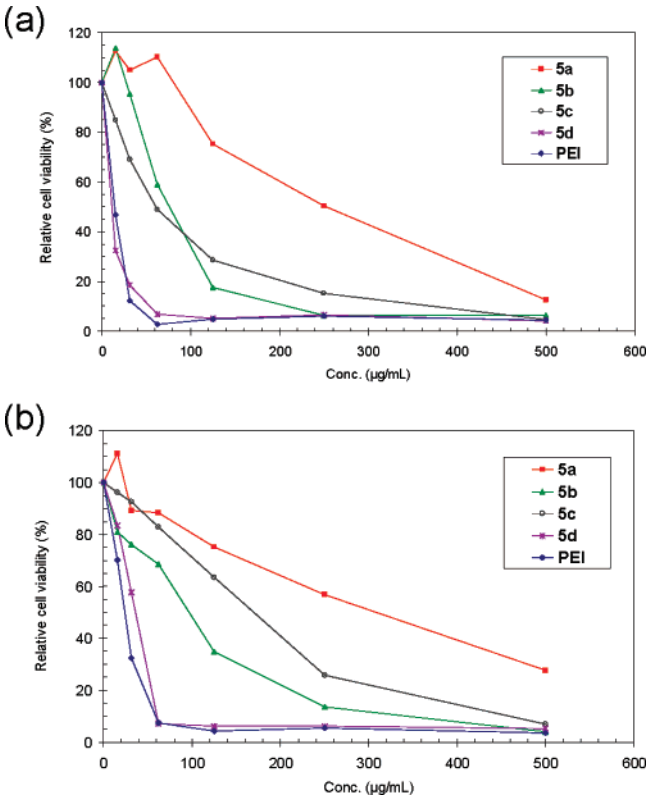

Figure 7. Cell viability of cationic polyrotaxanes in (a) HEK293 and (b) COS7 cells in comparison with PEI (25 kDa).

still be identified under AFM while small and compact nanoparticles were formed at the same time. In comparison to this partial condensation at a N/P ratio of 2, the same amount of pDNA could be tightly packed and completely formed pDNA complexes in the form of spherical nanoparticles at a N/P ratio of 10.

3.4. Cytotoxicity of Cationic Polyrotaxanes. Cytotoxicity is one of the most important factors to be considered in selecting polymeric materials as gene carriers. Figure 7 shows the results of in vitro cytotoxicity studies of cationic polyrotaxanes in two cell lines (HEK293 and COS7) using a MTT assay. As shown in Figure 7, all of the cationic polyrotaxanes showed a dose-dependent effect on cytotoxicity. It is worth noting that the cationic polyrotaxanes with linear OEI chains exhibited less toxicity in both cultured HEK293 and COS7 cells than the PEI control. The slopes of the dose−response cytotoxicity curves were much steeper for PEI (25 kDa) than those for **5a**, **5b**, and **5c**. One possible reason is that the introduction of cyclodextrin and copolymer results in the lower density of amino groups and the high density of amino groups is always considered as an important factor leading to high cytotoxicity of PEI.[34] Likewise, the cytotoxicity of **5d** was similar to that of PEI (25 kDa), which can also be attributed to its higher density of amino groups because **5d** was grafted with higher-MW branched OEI-14. These results also appeared to be supported by the calculated LD_{50} values: In COS7 cell lines, the LD_{50} value of PEI (25 kDa) was less than 25 μg/mL, while those of cationic polyrotaxanes **5a**, **5b**, **5c**, and **5d** were 97, 308, 170, and 36 μg/mL, respectively. A similar trend was also observed in HEK293 cell lines. It is noted that the cationic polyrotaxane concentrations used in our gene transfection experiments were mostly lower than 50 μg/mL, at which range the cationic polyrotaxanes and PEI (25 kDa) showed prominent different cytotoxicity. Therefore, the cytotoxicity of the gene carriers in this study may be an important factor affecting the gene transfection efficiency.

3.5. Gene Transfection Mediated by Cationic Polyrotaxanes. In vitro gene transfection efficiency of cationic polyrotaxane/DNA complexes was assessed using luciferase as a

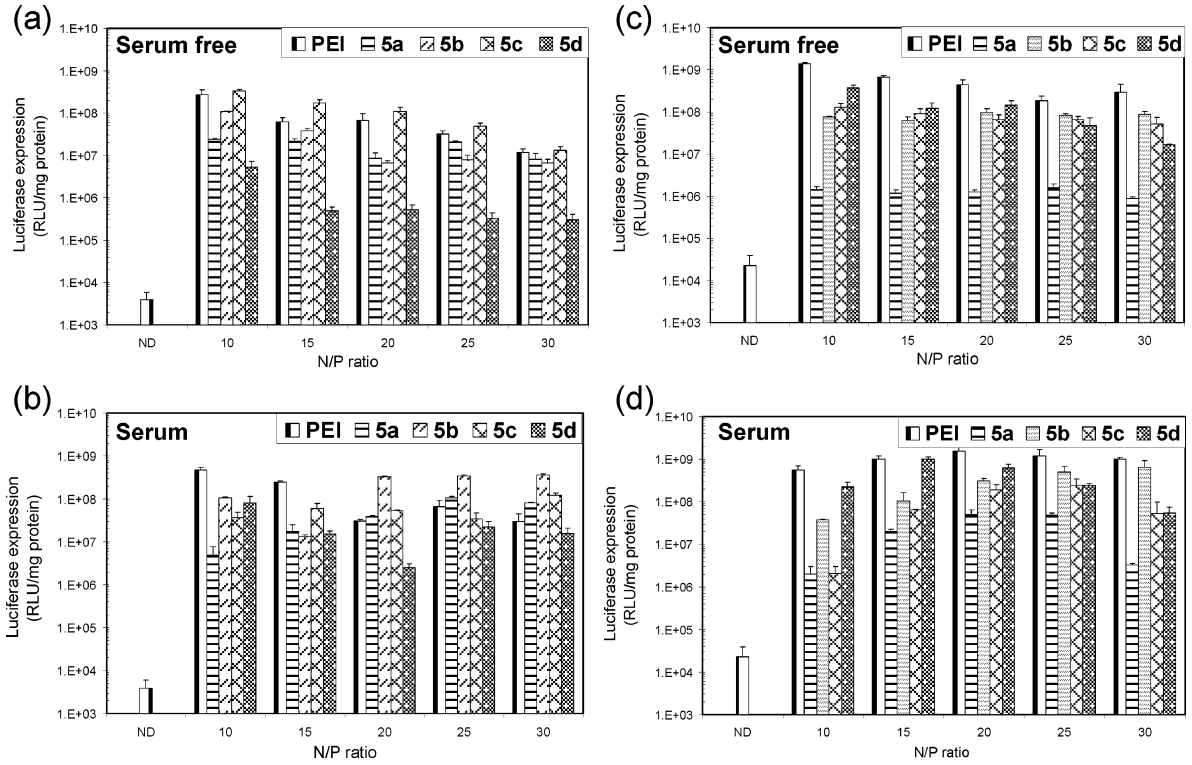

Figure 8. In vitro gene transfection efficiency of the cationic polyrotaxane/DNA complexes in comparison with that of PEI (25 kDa) or naked DNA (ND) in HEK293 cells in the (a) absence and (b) presence of serum and in COS7 cells in the (c) absence and (d) presence of serum. Data represent mean ± standard deviation ($n = 3$).

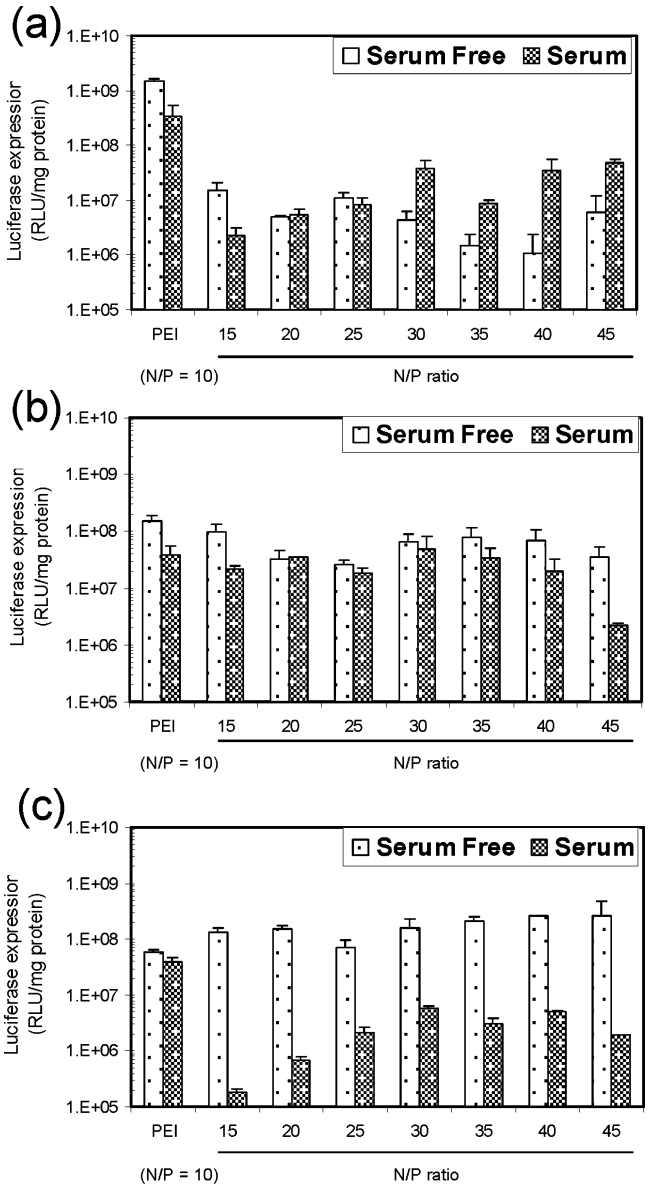

Figure 9. In vitro gene transfection efficiency of the cationic polyrotaxane **5b**/DNA complex in comparison with that of PEI (25 kDa) in (a) BHK-21 cells, (b) SKOV-3 cells, and (c) MES-SA cells in the absence and presence of serum. Data represent mean ± standard deviation ($n = 3$).

marker gene in HEK293 and COS7 cells. Figure 8 shows the gene transfection efficiency of cationic polyrotaxanes compared with those of branched PEI (25 kDa) and naked pDNA (ND) at various N/P ratios in the absence and presence of serum in HEK293 and COS7 cells.

In HEK293 cells (Figures 8a and 8b), the transfection efficiencies mediated by cationic polyrotaxanes were comparable to or even higher than those of branched PEI (25 K). When the transfection was conducted in the absence of serum, **5c** constantly exhibited the highest transfection efficiencies among the four cationic polyrotaxanes, which were also higher than the PEI control at low and high N/P ratios. From **5a** to **5c**, the transfection efficiency increased with an increase in the length of the OEI grafted to α-CD. However, **5d**, the one with longest OEI grafted, showed the lowest transfection efficiency. This is much different from PEI, where higher MW always results in higher transfection efficiency. When the transfection medium was supplemented with 10% FBS, **5b** exhibited the highest transfection efficiencies among the four cationic polyrotaxanes.

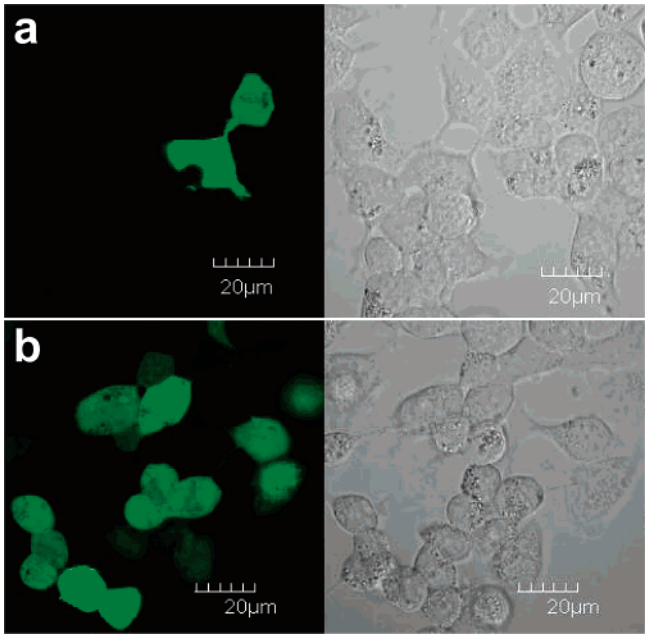

Figure 10. Confocal microscopy images of transfected HEK293 cells. The transfections were mediated by (a) cationic polyrotaxane **5c** and (b) PEI (25 K) at a N/P ratio of 10 in the absence of serum using GFP gene as a reporter gene. The same field of cells was observed by Nomarski optics (right panel) and by fluorescence microscopy (left panel) to visualize GFP expression.

The transfection efficiencies mediated by **5a**, **5b,** and **5c** increased with increasing N/P ratio and finally became much higher than those of PEI at high N/P ratios, while the transfection efficiency of PEI dropped at higher N/P ratios. Particularly, **5b** displayed an approximately 10 times higher transfection efficiency than that of the PEI control at N/P ratios of 20−30. Again, **5d** showed the lowest transfection efficiency among the four cationic polyrotaxanes except at a N/P ratio of 10.

In COS7 cells (Figures 8c and 8d), however, **5d** showed the highest transfection efficiency among the four cationic polyrotaxanes at low N/P ratios (10−20), while **5b** was the best for gene transfection at higher N/P ratios (25 and 30). Generally, the transfection efficiencies mediated by cationic polyrotaxanes were comparable to or slightly lower than those of branched PEI (25 kDa) in both reduced-serum medium and complete medium.

The in vitro transfection efficiencies of cationic polyrotaxane **5b** were also evaluated in three other cell lines including BHK-21, SKOV-3, and MES-SA cells at various N/P ratios, in comparison with those of branched PEI (25 kDa) at a N/P ratio of 10, at which branched PEI (25 kDa) usually exhibits the highest transfection efficiency. Like other transfection hosts such as HEK293 and COS7, the Syrian golden hamster kidney fibroblast cell line BHK-21 has been also widely used to evaluate in vitro gene transfection efficiency mediated by cationic polymers.[9] The human cell lines SKOV-3 (ovarian carcinoma) and MES-SA (uterus sarcoma) are derived from human tumor cells, which could serve as excellent candidates for tumor cell transfection investigations.[35,36] As shown in Figure 9, the gene transfection efficiencies of **5b** were dependent on the serum condition of the culture medium in different cell lines. In BHK-21 cells, the transfection efficiencies of **5b** improved with an increase in the N/P ratio in the serum condition, while its transfection efficiencies in the serum-free condition were lower at high N/P ratios. In SKOV-3 cells, the transfection efficiencies of **5b** at N/P ratios of 15−40 were similar to that

of the PEI control in the serum-free condition as well as in the serum condition. In MES-SA cells, the transfection efficiencies of **5b** were higher than that of the PEI control in the serum-free condition, while those of **5b** were much lower than that of the PEI control. Hence, when the cationic polyrotaxanes are properly designed with different compositions, densities of the amino groups, lengths of OEI grafted, and flexibilities of the main chains, the properties of the gene carriers may be altered to suit gene delivery in a wide range of different cells with high gene transfection efficiencies.

Finally, confirmation of the gene delivery capability of the cationic polyrotaxane **5c** was also obtained by fluorescence microscopy in contrast with that of PEI (25 kDa). Plasmid pEGFP-N1 encoding GFP was used to examine the GFP expression in HEK293 cells. As shown in Figure 10, strong fluorescence signals could be observed when transfection was mediated by either **5c** or PEI at a N/P ratio of 10. However, when the transfection was mediated by PEI, the GFP expression in HEK293 cells was stronger than that mediated by **5c**. In contrast, GFP expression could not be detected when the transfection was mediated by naked DNA, which was used as a negative control.

4. Conclusions

In the present study, four supramolecular cationic polyrotaxanes (**5a**, **5b**, **5c**, and **5d**) with multiple OEI-grafted cationic α-CD rings threaded and blocked on a P(EO-*r*-PO) copolymer chain have been successfully synthesized and characterized. In the cationic polyrotaxanes, approximately 12 cationic α-CD rings were threaded on a P(EO-*r*-PO) copolymer with a MW of 2370 Da and an EO/PO molar ratio of 4:1, while the cationic α-CD rings were grafted with linear OEI of a MW up to 423 Da for **5a, 5b**, and **5c** and with branched OEI of MW of 600 Da for **5d**. All four cationic polyrotaxanes could efficiently bind pDNA and form nanoparticles with sizes of 100−200 nm that were suitable for cell uptake. In vitro cytotoxicity studies showed that cationic polyrotaxanes **5a**, **5b**, and **5c** exhibited much lower cytotoxicity than high-MW branched PEI (25 kDa), while cationic polyrotaxane **5d** with branched OEI chains of higher MW (600 Da) exhibited similar cytotoxicity to high-MW branched PEI (25 kDa) in both HEK293 and COS7 cells. The cationic polyrotaxanes displayed high gene transfection efficiencies in a number of cell lines such as HEK293, COS7, BHK-21, SKOV-3, and MES-SA and showed strong cell type and serum condition dependency. In the serum condition, cationic polyrotaxane **5b** displayed an approximately 10 times higher transfection efficiency than that of the PEI (25 kDa) control at N/P ratios of 20−30. It is thought that the OEI-grafted α-CD rings were only located selectively on EO segments of the P(EO-*r*-PO) chain in the polyrotaxanes, while PO segments were free of complexation. Such structure increased the mobility of the cationic α-CD rings and the flexibility of the polyrotaxanes, which enhanced the interaction of the cationic α-CD rings with DNA and/or the cellular membrane.

Our studies have demonstrated that the new cationic polyrotaxanes have high gene delivery capabilities in a variety of cell lines. When properly designed, the structure, conformation, and composition of the cationic polyrotaxanes may be controlled to give gene carriers with different properties for a wide range of potential gene therapy applications.

Acknowledgment. We acknowledge the financial support from the Ministry of Education (Grant No. R-397-000-031-112) and the Institute of Materials Research and Eningeering, Singapore. We gratefully thank Professor K. W. Leong from Department of Biomedical Engineering, Duke University, for his valuable suggestions and helpful discussions.

Supporting Information Available. GPC profile of P(EO-*r*-PO) and ^{1}H NMR spectra of α-CD, P(EO-*r*-PO)−bisamine **2**, and α-CD-P(EO-*r*-PO) polyrotaxane **4**. This material is available free of charge via the Internet at http://pubs.acs.org.

References and Notes

(1) De Smedt, S. C.; Demeester, J.; Hennink, W. E. *Pharm. Res.* **2000**, *17*, 113−126.
(2) Park, T. G.; Jeong, J. H.; Kim, S. W. *Adv. Drug Delivery Rev.* **2006**, *58*, 467−486.
(3) Boussif, O.; Lezoualch, F.; Zanta, M. A.; Mergny, M. D.; Scherman, D.; Demeneix, B.; Behr, J. P. *Proc. Natl. Acad. Sci. U.S.A.* **1995**, *92*, 7297−7301.
(4) Zauner, W.; Ogris, M.; Wagner, E. *Adv. Drug Delivery Rev.* **1998**, *30*, 97−113.
(5) Kukowska-Latallo, J. F.; Bielinska, A. U.; Johnson, J.; Spindler, R.; Tomalia, D. A.; Baker, J. R. *Proc. Natl. Acad. Sci. U.S.A.* **1996**, *93*, 4897−4902.
(6) Dekie, L.; Toncheva, V.; Dubruel, P.; Schacht, E. H.; Barrett, L.; Seymour, L. W. *J. Controlled Release* **2000**, *65*, 187−202.
(7) Wang, J.; Mao, H. Q.; Leong, K. W. *J. Am. Chem. Soc.* **2001**, *123*, 9480−9481.
(8) Roy, K.; Mao, H. Q.; Huang, S. K.; Leong, K. W. *Nat. Med.* **1999**, *5*, 387−391.
(9) Hwang, S. J.; Bellocq, N. C.; Davis, M. E. *Bioconjugate Chem.* **2001**, *12*, 280−290.
(10) Davis, M. E.; Brewster, M. E. *Nat. Rev. Drug Discovery* **2004**, *3*, 1023−1035.
(11) Arima, H.; Kihara, F.; Hirayama, F.; Uekama, K. *Bioconjugate Chem.* **2001**, *12*, 476−484.
(12) Kihara, F.; Arima, H.; Tsutsumi, T.; Hirayama, F.; Uekama, K. *Bioconjugate Chem.* **2003**, *14*, 342−350.
(13) Yang, C.; Li, H. Z.; Goh, S. H.; Li, J. *Biomaterials* **2007**, *28*, 3245−3254.
(14) Wenz, G.; Keller, B. *Angew. Chem., Int. Ed. Engl.* **1992**, *31*, 197−199.
(15) Harada, A.; Li, J.; Kamachi, M. *Nature* **1992**, *356*, 325−327.
(16) Harada, A.; Li, J.; Kamachi, M. *Nature* **1994**, *370*, 126−128.
(17) Li, J.; Harada, A.; Kamachi, M. *Polym. J.* **1994**, *26*, 1019−1026.
(18) Fujita, H.; Ooya, T.; Yui, N. *Macromolecules* **1999**, *32*, 2534−2541.
(19) Li, J.; Li, X.; Zhou, Z. H.; Ni, X. P.; Leong, K. W. *Macromolecules* **2001**, *34*, 7236−7237.
(20) Li, X.; Li, J.; Leong, K. W. *Macromolecules* **2003**, *36*, 1209−1214.
(21) Nepogodiev, S. A.; Stoddart, J. F. *Chem. Rev.* **1998**, *98*, 1959−1976.
(22) Wenz, G.; Han, B. H.; Muller, A. *Chem. Rev.* **2006**, *106*, 782−817.
(23) Ooya, T.; Yui, N. *J. Controlled Release* **1999**, *58*, 251−269.
(24) Li, J.; Ni, X. P.; Leong, K. W. *J. Biomed. Mater. Res., Part A* **2003**, *65*, 196−202.
(25) Li, J.; Li, X.; Ni, X. P.; Wang, X.; Li, H. Z.; Leong, K. W. *Biomaterials* **2006**, *27*, 4132−4140.
(26) Hirose, H.; Sano, H.; Mizutani, G.; Eguchi, M.; Ooya, T.; Yui, N. *Langmuir* **2004**, *20*, 2852−2854.
(27) Yui, N.; Ooya, T. *Chem.—Eur. J.* **2006**, *12*, 6730−6737.
(28) Li, J.; Yang, C.; Li, H. Z.; Wang, X.; Goh, S. H.; Ding, J. L.; Wang, D. Y.; Leong, K. W. *Adv. Mater.* **2006**, *18*, 2969−2974.
(29) Ooya, T.; Choi, H. S.; Yamashita, A.; Yui, N.; Sugaya, Y.; Kano, A.; Maruyama, A.; Akita, H.; Ito, R.; Kogure, K.; Harashima, H. *J. Am. Chem. Soc.* **2006**, *128*, 3852−3853.
(30) Li, J.; Li, X.; Toh, K. C.; Ni, X. P.; Zhou, Z. H.; Leong, K. W. *Macromolecules* **2001**, *34*, 8829−8831.
(31) Khan, A. R.; Forgo, P.; Stine, K. J.; D'Souza, V. T. *Chem. Rev.* **1998**, *98*, 1977−1996.
(32) Mansouri, S.; Cuie, Y.; Winnik, F.; Shi, Q.; Lavigne, P.; Benderdour, M.; Beaumont, E.; Fernandes, J. C. *Biomaterials* **2006**, *27*, 2060−2065.

(33) Kunath, K.; von Harpe, A.; Fischer, D.; Peterson, H.; Bickel, U.; Voigt, K.; Kissel, T. *J. Controlled Release* **2003**, *89*, 113−125.
(34) Merdan, T.; Kopecek, J.; Kissel, T. *Adv. Drug Delivery Rev.* **2002**, *54*, 715−758.
(35) Xie, X.; Ye, D. F.; Chen, H. Z.; Lu, W. G.; Fu, Y. F.; Cheng, B.; Zhu, H. *Gynecol. Oncol.* **2004**, *92*, 578−585.
(36) Bonsted, A.; Engesaeter, B. O.; Hogset, A.; Maelandsmo, G. M.; Prasmickaite, L.; D'Oliveira, C.; Hennink, W. E.; Steenis, J. H.; Berg, K. *J. Gene Med.* **2006**, *8*, 286−297.

BM700472T